FRACTURE TOUGHNESS AND FATIGUE CRACK GROWTH TESTS OF FRICTION STIR WELDED PLATES

By

Siti Nur Farhin Mokhtar

Dissertation submitted in partial fulfillment of
the requirements for the
Bachelor of Engineering (Hons)
(Mechanical Engineering)

JANUARY 2012

UNIVERSITI TEKNOLOGI PETRONAS
BANDAR SERI ISKANDAR
31750 TRONOH
PERAK DARUL RIDZUAN

CERTIFICATION OF APPROVAL

FRACTURE TOUGHNESS AND FATIGUE CRACK GROWTH TESTS OF FRICTION STIR WELDED PLATES

by

Siti Nur Farhin Mokhtar

A Dissertation submitted to the

Department of Mechanical Engineering

Universiti Teknologi PETRONAS

in partial fulfillment of the requirement for the

BACHELOR OF ENGINEERING (Hons)

(MECHANICAL ENGINEERING)

Approved by,

(Dr. Azmi Abdul Wahab)

Dr. Azmi Abd Wahab
Lecturer
Mechanical Engineering Department
Universiti Teknologi PETRONAS
Bandar Seri Iskandar, 31750 Tronoh
Perak Darul Ridzuan, Malaysia.

UNIVERSITI TEKNOLOGI PETRONAS

TRONOH, PERAK

JANUARY 2012

CERTIFICATION OF ORIGINALITY

This is to certify that I am responsible for the work submitted in this project, that the original work is my own except as specified in the references and acknowledgements, and that the original work obtained herein have not been undertaken or done by unspecified sources or persons.

SITI NUR FARHIN BINTI MOKHTAR

ABSTRACT

Friction stir welding has been demonstrated as a viable replacement to conventional fusion welding in various engineering applications. In most cases, the suitable welding parameters were selected based primarily on the tensile tests performed on welded test joints. In this project, a study on fracture toughness and fatigue crack growth of friction stir welded aluminium plates was performed. Two types of tests were conducted according to ASTM Standard Test Method E647-08 for fatigue crack growth and E399-08 for fracture toughness. The objectives of the project were to perform Fracture Toughness and Fatigue Crack Growth test on Friction Stir Welded aluminium plates, determining the plane strain fracture toughness K_{IC}, establishing the rate of fatigue crack growth of the A6061 welded plates, and comparing those properties with non-welded A6061 plates. Friction stir welding was conducted using CNC milling machine with a tool pin of 8 mm length, pin diameter of 6 mm and shoulder diameter of 12 mm at 1600 rpm tool rotational speed, 12 mm/min weld speed and 12s dwell time. The results indicated that the friction stir welded plates exhibited lower fracture toughness and higher cracks propagation rate than non-welded plates.

ACKNOWLEDGEMENT

بسم الله الرحمن الرحيم

With the name of Allah
The Most Gracious The Most Merciful

First of all, my deepest gratitude to Allah SWT, the Lord of Universe for His blessings and guidance for being able to accomplish my Final Year Project entitled "Fracture Toughness and Fatigue Crack Growth Tests of Friction Stir Welded Plates". Special thanks and appreciation dedicated to my parents and family members for their support and encouragement towards me in completing this project.

First and foremost, I wish to thank my Supervisor, Dr Azmi Abdul Wahab for his valuable advice, continuous guidance, motivational support and positive criticisms that has helped me a lot since the start of this project until the completion of this project. He has driven me beyond my preconceived limits, which enabled me to discover my new strengths and capabilities. This Final Year Project has given me lots of useful knowledge and experiences.

A high appreciation to all Mechanical Department technicians that involved directly and indirectly in this project especially Lab Technician for Amsler Universal Test Mechanical (UTM) machine, Mr Paris Said, Lab Technical for Electron Discharged Machining machine, Mr Zamil Khairuddin and Lab technician for CNC Milling machine, Mr Shaiful Hisham Samsudin for their assistance. They have been a great help during the whole experimental process. This project would never been a success without their support and technical assistance.

Finally, thank you to Mechanical Engineering Department, Examiners and Coordinators of the Final Year Project for making this program a success. They have been very helpful, tolerant and considerate throughout completing this project. Thank you to all parties involved for their contribution, guidance and support until the completion of this project.

Table of Contents

List of Figures

List of Tables

CHAPTER 1
INTRODUCTION

1.1 Background of study

Friction stir welding (FSW), which was introduced by The Welding Institute in 1991, has emerged as a promising alternative to conventional fusion welding. It bonds the two (or more) plates by using a rapidly rotating cylindrical-shouldered tool with a threaded or non-threaded probe that travels along the joint line at a constant speed. The friction heat generated softens the stirred material without reaching the melting point of the alloy being joined (Sivashanmugan, Ravikumar, Rao, Muruganandam, & Kumar, 2010).

In engineering design, the most basic concern to avoid structure failure is that the stress applied on the component must not exceed the material's strength. Nevertheless, in the presence of a crack, the component may be weakened and failure may occur at a much lower stress than normal. Fracture toughness is a fundamental material property that depends on critical stress and crack length for crack propagation under static load. Plane-strain fracture toughness, K_{IC} is the crack-extension resistance under conditions of crack-tip plane strain in Mode I (opening mode) for slow rates of loading under predominantly linear-elastic conditions and negligible plastic-zone adjustments. It is characterized by the material's resistance to fracture in a neutral environment in the presence of a sharp crack under essentially linear-elastic stress and severe tensile constraint (ASTM, 2008). On the other hand, fatigue crack growth (FCG) is crack propagation caused by cyclic loading. Basically, the FCG test is designed to determine the rate of crack. These are among the important variables that must be considered in design involving welding.

In this study, the interest is to investigate these mechanical properties of FSW welded plates and compare them with the properties of non-welded A6061 aluminium plates. The tests involved are Plane-Strain Fracture Toughness and Fatigue Crack Growth tests which followed the American Society for Testing and Materials (ASTM) Standards E399-08 and E647-08 (ASTM, 2008). As recommended by both standards,

the sample plates were fabricated into Compact Tension (CT) specimens. There are actually three ASTM specimen configurations which are the Compact Tension (CT), Three-Point Bend, and C-Shaped. C-Shaped specimen is designed for fracture toughness testing of cylinders and thick bars. The CT and Three-Point Bend specimen are used for general purposes. CT is a specimen configured with a single edge-notch which is loaded in tension. CT sample is recommended because it requires the least amount of test material compared to the Three-Point Bend specimen (ASTM, 2008).

1.2 Problem Statement

In Friction Stir Welding (FSW), the interaction of a non-consumable rotating tool with the components being welded creates a welded joint through frictional heating and plastic deformation at a temperature below the melting temperature of the alloys that are being joined. The advantages offered by FSW have attracted many researchers who are now focusing on development of the technique especially in the application of lightweight alloys. Despite the widespread interest in the possibilities offered by FSW, data concerning the mechanical behavior of joints obtained using this process is still scarce. Research work on fatigue crack growth data from the weld zone is required to provide tools to assess the damage tolerance issues (Moreira, Jesus, Ribeiro, & Castro, 2008).

The microstructure, mechanical strength and their relation with FSW process parameters have been extensively studied in the past few years especially in the case of lightweight alloys such as aluminum alloys. Most of mechanical properties of the FSW are measured based on static mechanical testing such as static tensile tests and hardness tests. However, there are very few data that is available at present on fracture mechanics, or tests in the presence of crack.

In reality, cracks or crack-like flaws occur frequently. Various periodic inspections of large commercial aircraft frequently reveal cracks that sometimes are critical and must be repaired. They also commonly occur in other critical components such as in ship structures, bridge structure, pressure vessel, piping, heavy machinery, vehicle and nuclear reactors. Presence of cracks can significantly reduce the strength

of an engineering component so that it can fail at stresses below the material's yield strength. Therefore, the interest of this study is to investigate the behavior of the FSW welded aluminum plates in the presence of cracks.

1.3 Objectives of study

The main objectives of the study are to perform Fracture Toughness (FT) and Fatigue Crack Growth (FCG) test on the Compact Tension (CT) plates to determine the plain-strain fracture toughness, K_{IC} and the rate of crack propagation on FSW plates, and evaluate the performance of Friction Stir Welding at the chosen welding parameters and pin design.

Currently the selection of FSW parameters are mainly based on visual inspection of the weld, and basic mechanical tests such as tensile tests and hardness tests. It is anticipated that this work would lay the groundwork to further optimize the welding parameters to account for flaws that might be inherent in the FSW process, and also include the effects of cyclic loading in the parameter optimization process.

1.4 Scope of study

This study involved Fracture Toughness and Fatigue Crack Growth tests on non-welded (NW) and friction stir welded (FSW) A6061 plates with respect to ASTM Standards E399-08 and ASTM E647-08 using CT specimens. Single-pass FSW butt joints were prepared using CNC milling machine at 1600 rpm tool rotational speed, 12 mm/min weld speed and 12 s dwell time using a tool pin of 8 mm length, pin diameter of 6 mm and shoulder diameter of 12 mm. The tests were conducted using the Amsler Universal Testing Mechanical (UTM) coupled with other CT specimen accessories such as clevises, pins, extensometer, and extensometer holder.

1.5 Relevancy of Project

By doing this study, we can analyze the mechanical behaviour of FSW welded material with cracks presence in the engineering component such as its resistance to failure in terms of the yield strength which is very crucial in engineering design. This is to assure safety and avoid structural failure caused by unpredictable crack growth.

1.6 Feasibility of Project

Final year project for mechanical engineering students is obligatory to be completed within two semesters. The project commences with background study, research work and laboratory works in the eight months' time of the first semester. It is assumed that the project is feasible within the scope and time frame if there was no issue with regard to equipment function and material availability.

CHAPTER 2
LITERATURE REVIEW

2.1 Properties of Aluminium Alloy A6061-O

Aluminium is a silverish white metal that relatively light metal compared to steel, nickel, brass and copper. Aluminium is also easily machined. The alloy designation is based on a four digit international code where:

1. The 1st digit referring to the principal alloying constituent;
2. The 2nd digit referring to variations of the initial alloy;
3. The 3rd and 4th digits referring to individual alloy variations.

The temper designation code corresponds to different strengthening techniques. The chemical composition, mechanical properties and physical properties of A6061 are given in Table1 and Table 2, respectively (Kaiser Aluminium, 2010).

Table 1: Chemical composition of A6061

Component	**Wt %**	**Component**	**Wt %**
Mg	0.8 - 1.2	**Ti**	Max 0.15
Cu	0.15 - 0.4	**Fe**	Max 0.7
Cr	0.04 - 0.35	**Mn**	Max 0.15
Si	0.4 - 0.8	**Al**	Bal
Zn	Max 0.25		

Table 2: Typical Mechanical properties of A6061

Yield strength (MPa)	**Ultimate strength** (MPa)	**Elongation** (%)	**Hardness** (VHN)	**Modulus of Elasticity** (GPa)
241	145	25	65	68.3

2.2 Plane Strain Fracture Toughness

The term fracture toughness is a property that indicates the amount of stress required to propagate a preexisting flaw. It is a very important material property since the occurrence of flaw is not completely avoidable in processing, fabrication, or service of a material/component (Erdogan, 2000). In common situations, a small flaw (that is initially present) develops into a crack and then grows until it reaches the critical size, where the applied load can cause sudden catastrophic failure. A cracked body can be loaded in any one or combination of three typical modes of fracture (as illustrated in Figure 1). Mode I is an opening mode caused by displacements of the crack surfaces that are perpendicular to the plane of the crack. Mode II is a sliding mode caused by in-plane shear and Mode III is a tearing mode caused by out-of-plane shear. However, most practical applications involve Mode I (Dowling, 1999).

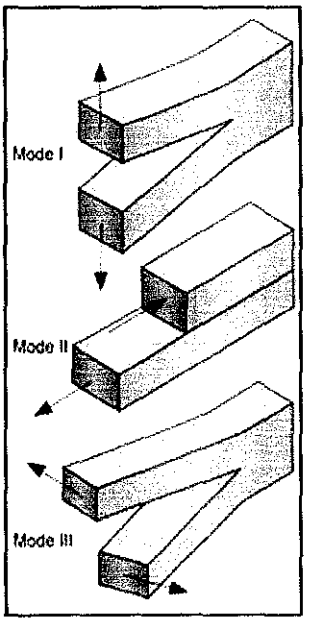

Figure 1: Basic loading modes: Mode I – opening, Mode II – sliding mode, and Mode III – tearing mode (Dowling, 1999).

Stress intensity factor, K characterizes the severity of the crack situation by considering its crack size a, loading stress σ, and structural geometry B. The equation for stress intensity factor, K can be presented by $K = \sigma\sqrt{\pi a B}$. In defining K, the material is assumed to behave in a linear-elastic manner where the relationship between load and displacement is linear according to Hooke's Law. As long as K is

below that a critical value, K_C, the material can avoid brittle fracture. K_C is a material property referred to as fracture toughness. Values of K_C vary widely for different materials and are affected by temperature and loading rate (Dowling, 1999).

The plane-strain fracture toughness is a material property when displacements of all points in the body are parallel to a given plane and the values of these displacements do not depend on the displacement perpendicular to the plane. When plane strain is zero, $\varepsilon_z = 0$ in which brittle fracture occurs. This only occur when the K_I value characterize the magnitude of the stress field near the crack tip while K_{IC} is can be presented below as a relationship between critical stress for crack growth σ_c, and crack length a:

$$K_{Ic} = Y\sigma_c\sqrt{\pi a}$$

where Y is dimensionless parameter and a is the crack length for edge cracks or one half crack length for internal crack.

2.3 Friction Stir Welding (FSW)

The FSW technique was invented in 1992 by The Welding Institute (TWI). It has been widely used in the aerospace, shipbuilding, automobile industries and in many applications of commercial importance. It is also more advantageous compared to the commonly used fusion welding technique because of very low distortion, free from porosity, lack of fumes, and does not require consumables, special surface treatments or shielding gas requirements.

In FSW, a cylindrical-shouldered tool with a profiled threaded or unthreaded probe (nib or pin) will be rotated at a constant speed into the joint line between two pieces of sheet or plate as illustrated in the Figure 2 (Kumbhar & Bhanumurthy, 2008). The generated frictional heat will cause the stirred material to soften without reaching its melting point, allowing the probe to transverse along the joint. The welding of the material is facilitated by severe plastic deformation in the solid state, involving dynamic recrystallization of the base material. FSW can be carried out easily using a vertical milling machine (Kumbhar & Bhanumurthy, 2008).

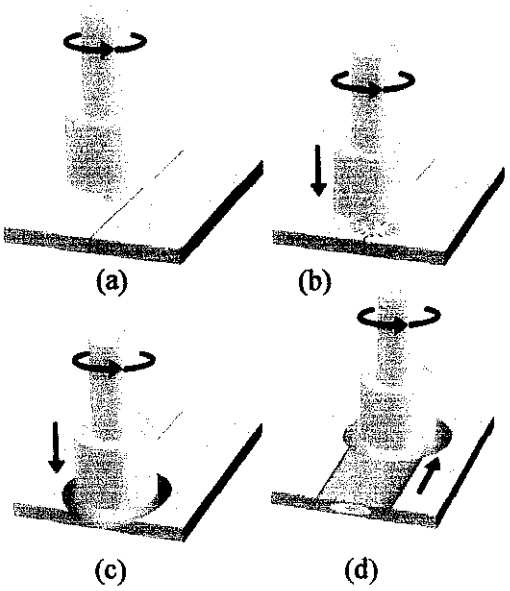

Figure 2: Processes in friction stir welding: (a) rotating tool prior to penetration into the butt joint; (b) tool probe makes contact with the part, creating heat; (c) shoulder makes contact, restricting further penetration while expanding the hot zone; and (d) part moves under the tool, creating a friction-stir-weld nugget (Mahoney, Rhodes, Flintoff, Spurling, & Bingel,

2.4 Compact Tension C(T) Specimen

2.4.1 Specimen Configuration and Size

The dimensions of C(T) specimen must be within the tolerances shown in Figure 3. The thickness, B and width, W may be varied independently within the recommended following limits based on specimen buckling and through-thickness crack-curvature consideration (ASTM, 2008):

i. The thickness is within the range $\frac{W}{20} \le B \le \frac{W}{4}$

ii. a is measured from the line connecting the bearing points of force application.

iii. The machined notch, a_n in the C(T) specimen be at least $0.2W$ in length

While, the minimum in-plane specimen size required is that the specimen must be prodominantly elastic at all values of applied force. The following requirement must be fulfilled: $(W-a) \ge \left(\frac{4}{\pi}\right)\left(\frac{K_{MAX}}{\sigma_{YS}}\right)^2$, where $(W-a)$ is minimum recommended ligament size and σ_{YS} is the 0.2% offset yield strength of the material.

The ratio of yield strength to elastic modulus may be used for selecting a specimen size.

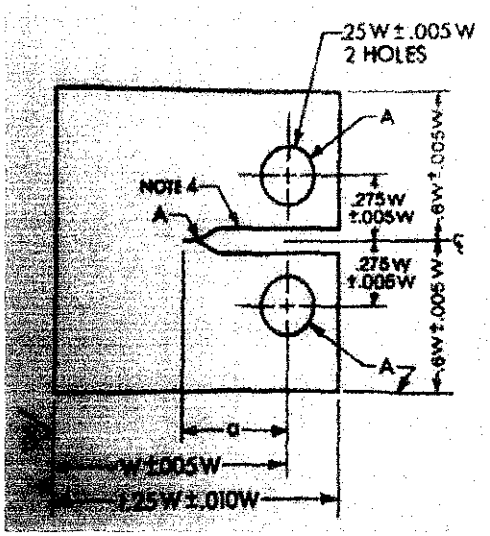

Figure 3: Compact tension specimen in standard proportion and tolerance

2.4.2 Specimen Fabrication

Machining to the required specimen dimension is a crucial part in the preparation of the tests because it will affect the accuracy of the crack growth measurements. In preparing deep edge-notch, Table 3 below lists the recommended equipments.

Table 3: Equipments for notch preparation (ρ, notch root radius)

Equipment	**Recommended for:**
Electric Discharge Machining (EDM)	$\rho < 0.25$ mm (0.010 in), high-strength steels ($\sigma_{ys} \geq 1175$ MPa/170 ksi), titanium and aluminium alloys
Mill or broach	$\rho < 0.25$ mm (0.003 in) alloy, low medium-strength steels ($\sigma_{ys} \geq 1175$ MPa/170 ksi), aluminium alloys
Grind	$\rho < 0.25$ mm (0.010 in), low and medium-strength steels
Sawcut	Alluminium alloys only

2.5 Standard Test Method for Measurement of Fatigue Crack Growth Rates

The standard test method for the measurement of fatigue crack growth (FCG) rates is ASTM E647-08. This test method determines the fatigue crack growth rates from near threshold to stress-intensity factor of unstable rapid growth, K_{max} (refer to Figure 4). The test method can be conducted to establish the following:

1. The fatigue crack growth characteristic on the life of a material
2. The material selection criteria and inspection requirements
3. The effects of metallurgical, fabrication, environmental and loading variables on fatigue crack growth

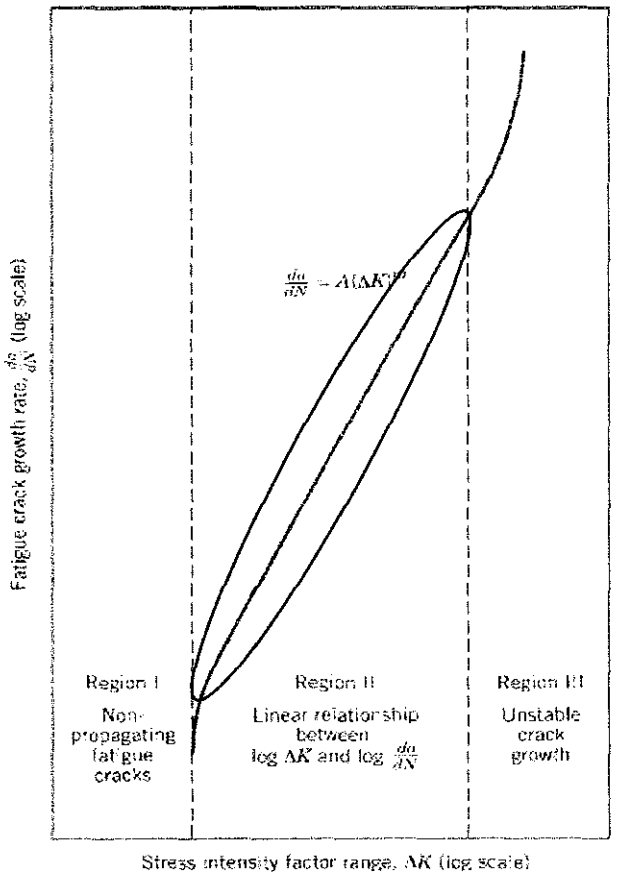

Figure 4: Paris Law curve (in log scale) obtained from "How fatigue crack ignition and growth properties after material selection and design criteria", *Metals Engineering Quarterly*, Vol. 14, No.3, 1974

The test involves cyclic loading of notched specimens in fatigue. The growth of the crack is recorded in terms of the numbers of cycles required for the crack length to reach each of ten to twenty or more different values. These data are then subjected

to numerical analysis to determine the rate of crack growth which expressed as a function of the stress-intensity factor range, ΔK (ASTM, 2008). The relationship is presented as:

$$\frac{da}{dN} = C(\Delta k)^m$$

where $\frac{da}{dN}$ is the cyclic crack growth rate, C is a constant and m is slope on the log-log plot representing the crack growth rate.

This relationship of cyclic crack growth rate and stress-intensity factor range provides results that are independent of planar geometry as long as specimen thickness remains constant. The presence of residual stresses however, may influence measurement of growth rate. But it can be reduced by selecting:

1. A small ratio of specimen dimensions, B/W
2. A specimen shape that can display significant crack-mouth movement
3. A symmetrical specimen configuration

2.6 Standard Test Method for Linear-Elastic Plane-Strain Fracture Toughness K_{IC} of Metallic Materials

ASTM Standard E399-08 is the standard test method for linear-elastic Plane-Strain Fracture Toughness, K_{IC} of metallic material which covers the determination of the material K_{IC} values by slow loading of fatigue precracked specimens. Force versus crack-mouth opening displacement (CMOD) is digitally or autographically recorded using a Double-Cantilever Clip-In Displacement gage and computer data acquisition system.

2.6.1 Fatigue Precracking

Before conducting the FT test, specimen has to be precracked first. Fatigue precracking is to produce a sharp crack that is well enough to provide a satisfactory measurement of K_{IC}. The dimensions of the notch and the precrack, and the sharpness of the precrack must meet certain conditions. It is produced by apply cyclic loading which usually 10,000 to 1,000,000 cycles at the notched specimen at a loading ratio of

10. Number of cycles depends on the specimen size, notch preparation and cyclic stress-intensity factor level. The stress-intensity factor, K_{max} during any stage of fatigue crack growth must not exceed 80% of the estimated K_{IC} except at the final precracking stage where the maximum stress-intensity factor must be less than 60% (ASTM, 2008).

2.6.2 Role of Material Thickness

Different absolute size of specimens produces different value for K_I because the stress states adjacent to the flaw changes with the specimen thickness B until the thickness exceeds some critical dimension. At the point where the thickness exceeds some critical dimension, the value of K_I becomes relatively constant. This value of K_I is a true material property which is called as plane-strain fracture toughness, K_{IC}. The stress intensity, K_I represents the level of stress at the tip of the crack and K_{IC} is the highest value of the intensity that a material can withstand without fracture under the plane-strain conditions. Plane-strain is a condition where the displacements of all points in body are parallel to a given plane and not depending on the distance perpendicular to the plane.

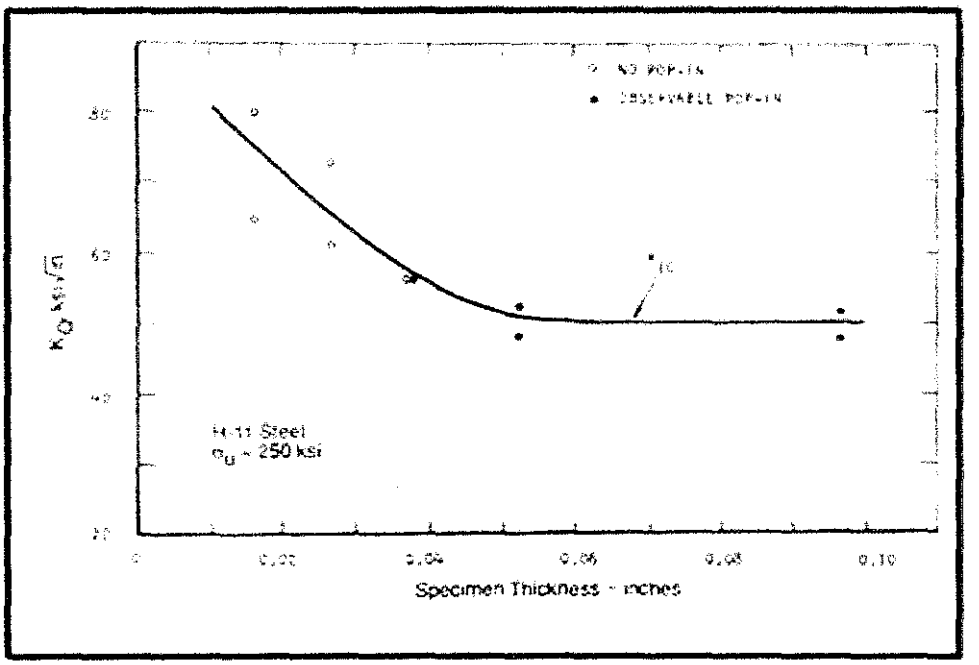

Figure 5: Influence of thickness in fracture toughness test (Dowling, 1999)

2.6.3 Plain-Strain Fracture Toughness Testing

Fracture toughness test covers the determination of plane-strain fracture toughness (K_{IC}) of metallic materials by increasing-load test of fatigue precracked specimens. The validity of the K_{IC} depends upon the establishment of a sharp-crack condition at the tip of the fatigue crack. Load is applied either in tension or three-point bending. In performing the test and determining the accurate K_{IC}, it is required that $B \geq 2.5\left(\frac{K_{IC}}{\sigma_Y}\right)^2$ where B is the critical thickness that produces a condition where plastic strain energy at the crack tip is minimal, K_{IC} is the fracture toughness of the material and σ_{YS} is the yield stress of the material. If the material fracture toughness is unknown, the material thickness should be based on a prediction of the fracture toughness. If the fracture toughness value does not satisfy the requirement of the above equation, the test should be repeated using a thicker specimen. When the test failed to meet the thickness and other test requirements, the fracture toughness value produced is designed as K_C at that particular thickness.

2.6.4 Significance of Plane-Strain Fracture Toughness

K_{IC} values can be used to predict the critical crack length, a_c at a given applied stress and the critical stress value, σ_c at a given crack length found in a component. By knowing these variables, the probability of having unexpected fracture can be reduced.

Critical crack length at applied stress:

$$a_c = \frac{1}{\pi}\left(\frac{K_{IC}}{\sigma Y}\right)^2$$

Where,

a_c is the critical crack length for edge crack (or one half crack length for internal crack)

K_{IC} is the fracture toughness of the material

Y is the coefficient of sample geometry

σ is the critical stress value at given crack length

Critical stress value when the crack length for edge crack (or one half crack length for internal crack) are known:

$$\sigma_C \leq \frac{K_{IC}}{Y\sqrt{\pi a}}$$

Where,

σ_c is the critical stress to a component

K_{IC} is the fracture toughness of the material

Y is the coefficient of sample geometry

a is the crack length for edge crack or one half crack length for internal crack

2.7 Summary of Related Literature

Two related articles are discussed in brief in this section. The first article by Moreira et al investigated fatigue crack growth behavior of friction stir butt welds of 3 mm thick 6082-T6 aluminium alloy. FCG curves were determined for different location of weldments: base material (BM), welded material (WM) and heat affected zone (HAZ). In their work, the friction stir welding were performed at 800 mm/min weld speed, 2^0 pitch angle and 1500 rpm rotating speed using a probe with 6 mm diameter threaded pin and 15 mm diameter shoulder. In order to understand the effect of welding process, monotonic tensile tests were carried out, followed by Vickers microhardness tests, and Scanning Electron Microscopy (SEM) observations carried out on the fracture surfaces. Their results showed that the WM yields lower yield stress and ultimate tensile stress than BM as well as lower elongation and hardness. As observed, failures occurred near the weld edge line. It was verified that the WM has better crack propagation resistance in comparison to HAZ and BM (Moreira, P., Jesus, A., Ribeiro, A., Castro, P., 2008).

The next article by Pirondi et al focused on the evaluation of fracture toughness and fatigue crack growth behavior of butt weld joints in A6061 aluminium alloy reinforced with 20% volume of Al_2O_3 particles (designated W6A20A) and A7005 aluminium alloy reinforced with 10% volume of Al_2O_3 particles (designated W7A10A). In this work, FSW butt joints were manufactured using a FSW probe made of Ferro-Titanit with a 20 mm diameter shoulder and 8 mm pin length. The parameters of the welding process were 600 rpm rotating speed and 300 mm/min

welding speed. Side grooves were machined in specimens for fracture test to keep plane strain conditions. FCG tests were conducted at $R = K_{min}/K_{max}$ equal to 0.1 and 0.5 at 10 Hz frequency under constant load amplitude. Metallographic and fractographic analysis were also conducted in order to understand the behavior of those materials. Their results indicated that the FT of the FSW joint is about 25% lower than the non-welded material for W6A20A and about 10 - 20% higher for W7A10A (Pirondi, A., Collini, L., Fersini, O., 2008)

CHAPTER 3
METHODOLOGY

3.1 Project workflow

The project workflow, shown schematically in Figure 6, started with preliminary research to understand the background of the project for the first few weeks before additional more in-depth literature review were carried out. In this stage, more detailed information was gathered regarding FSW technique, CT specimen dimension, and fracture toughness and fatigue crack growth test methods. Next, the sample preparation and testing was carried out to obtain the necessary data for analyses.

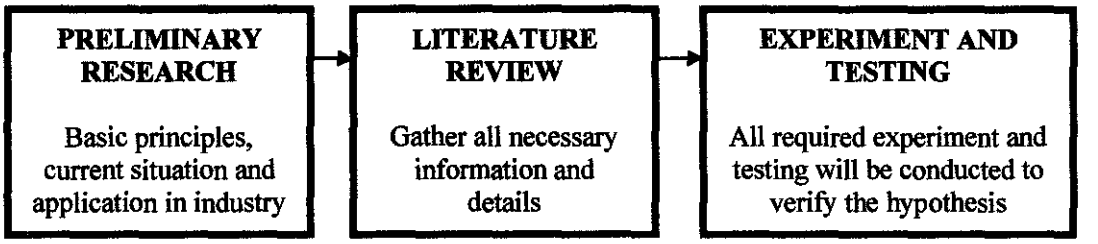

Figure 6: Project workflow

3.2 Tools Required

The experimental process involved the utilization of the following equipment or tools, which are listed in Table 4. The functions of the main equipment and tools used are as follows:

i. **CNC Milling machine**
   – to prepare FSW welded plates;

ii. **EDM Wire Cut machine**
   – to cut the aluminium plates into CT specimen;

iii. **Universal Testing Machine (UTM)**
   – to conduct the tests; applying cyclic loading to the specimen;

iv. **Extensometer**

– to measure the crack opening displacement as the cyclic loading is applied;

v. **Clevises and Pins**

– to hold the specimen when testing;

vi. **Dye penetrant liquid**

– to predict the crack length in fatigue precracking stage.

Table 4: List of equipment used

Laboratory Tasks	Materials, Equipment & Tools
Sample preparation	AutoCAD 2004, H13 non-threaded welding tool, Drill machine, Hammer, CNC Milling machine, EDM Wire Cut machine, A6061 Aluminium plates
Extensometer calibration	Retort stand and clamp, Micrometer, Caliper, and Extensometer, clip gauge
Fatigue precracking, Fracture Toughness and Fatigue Crack Growth Tests	Extensometer, Extensometer holder, clevises, pins, Amsler Universal Test Mechanical, Compact Tension sample plates, clip gauge, Dye Penetrant liquid, Caliper

3.2.1 Experimental Process

The overall flow of the project activities is summarized in Figure 7 and 8 below.

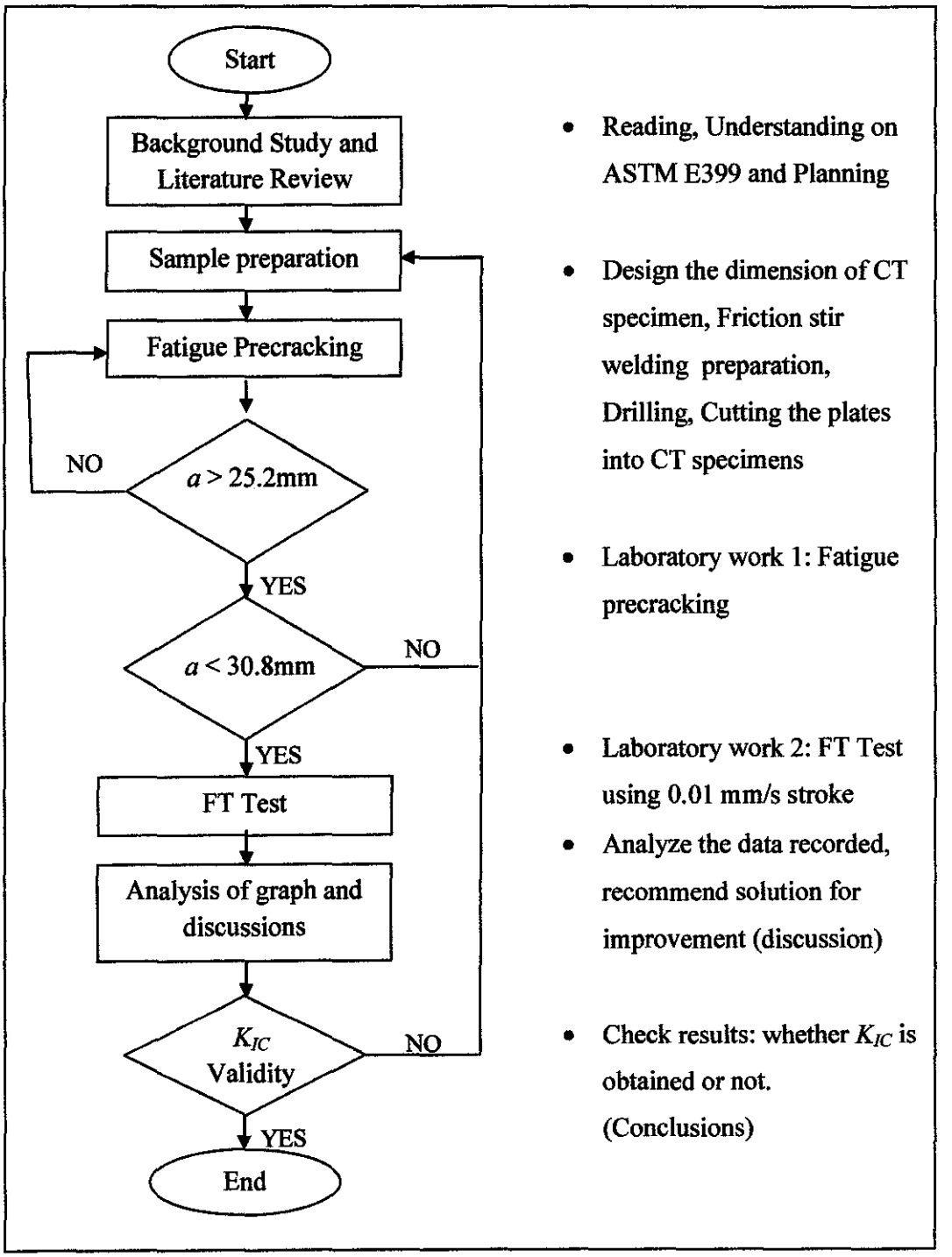

Figure 7: Flow chart of the FT test

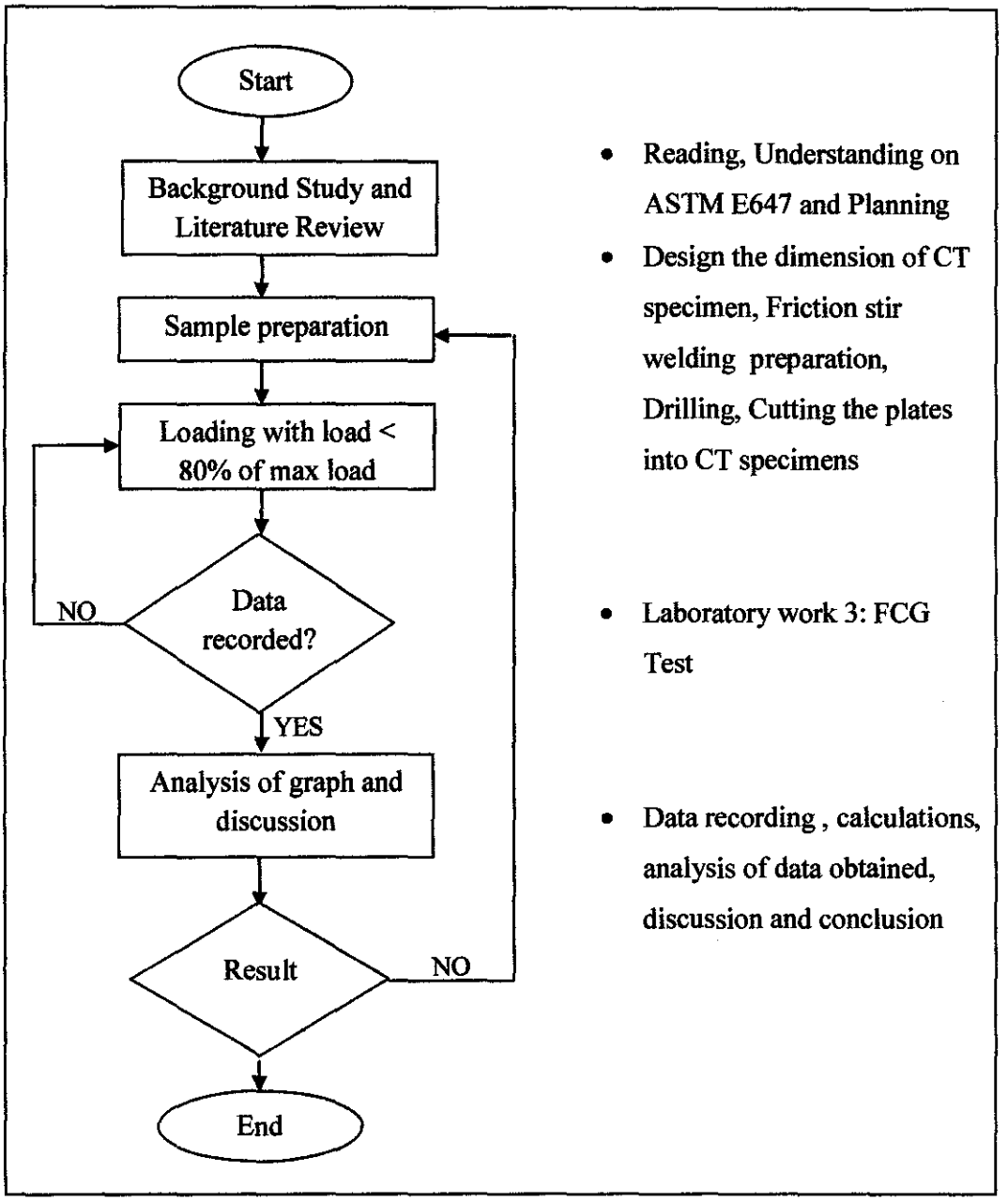

Figure 8: Flow chart of the FCG test

3.2.2 Fracture Toughness Test

A fatigue precracking task is the first step in the Fracture Toughness test where cyclical loading is applied to the notched specimen with loading ratio (min/max) of 0.1 for a number of cycles (usually 10,000 to 100,000 cycles) in stages to produce a sharp notch. It is one of ASTM requirements. Number of cycles depends on specimen size, notch preparation and stress intensity level.

The maximum stress-intensity factor (K_{max}) during any stage must not exceed 80% of the K_Q value except for the final stage of fatigue precracking, where K_{max} must not exceed 60% of the K_Q value. In this study, the fatigue precracking task is divided into two stages where the total crack length will reach at least 20 mm in stage 1 and 25.5 mm at stage 2. The crack length is measured from the centerline of the holes. The cyclic load is applied by increasing slowly from 40% to 80% for the Stage 1and 10% to 60% for the Stage 2. Appendix II shows the maximum cyclic load applied for the Stage 1 and Stage 2. The maximum cyclic load to be applied is calculated using equation below by assuming $K_Q = 50MPA\sqrt{m}$ for NW plate and $K_Q = 25MPA\sqrt{m}$ for FSW plate.

$$P_Q = \frac{K_Q B\sqrt{W}}{f(a/W)}$$

Where,

$$f\left(\frac{a}{W}\right) = \frac{(2+\frac{a}{W})\left[0.886 + 4.64\left(\frac{a}{W}\right) - 13.32\left(\frac{a}{W}\right)^2 + 14.72\left(\frac{a}{W}\right)^3 - 5.6\left(\frac{a}{W}\right)^4\right]}{\left(1-\frac{a}{W}\right)^{\frac{3}{2}}}$$

P_Q = Maximum load (kN),

K_Q = Portion of stress intensity factor,

a = crack length.

W = Width,

B = Thickness,

3.2.3 Fatigue Crack Growth Test

At crack growth rates greater than 10^{-8} m/cycle, the variability of $\frac{da}{dN}$ at a given ΔK is typically about a factor of two. It is a good practice to conduct replicate tests since the confidence in inferences drawn from the data increases with number of tests. When this is impractical, test should be planned to obtain regions of overlapping $\frac{da}{dN}$ versus ΔK data. In preparing for fatigue precracking, the equipment must be produced symmetrical force distribution with respect to the machined notch and K_{max} during

precracking is controlled to within ±5%. The fatigue precrack must also be not less than 0.10*B*, *h* or 1.0 mm.

3.3 Gantt Chart

The Gantt chart for Final Year Project semester 2 is shown in Table 4. Laboratory work involving preparation and actual running of the FT and FCG test dominates the schedule.

Table 5: Project Gantt chart

No	Activity / Week	1	2	3	4	5	6	7	Mid-SEM Break	8	9	10	11	12	13	14	15
1.	Trial testing - Calibration (Extensometer) - Precracking	■	■														
2.	Conduct trial tests		■	■	■					●							
3.	Conduct Friction Stir welding			■	■	■											
4.	**Laboratory work 1:** Sample preparation					■	■	■									
5.	**Laboratory work 2:** Fatigue precracking									■	■	■	■				
6.	**Laboratory work 3:** Fracture toughness test												■	■			
7.	**Laboratory work 4:** Fatigue Crack Growth test													■	■		
8.	Submission of soft bound and technical report													■	■	■	●
9.	Oral Presentation																●
10.	Submission of Project Dissertation (hard bound)																●

CHAPTER 4
RESULTS AND DISCUSSION

4.1 Sample Preparation

The tests in this study were conducted on plates fabricated into Compact Tension specimens. The Compact Tension specimens were designed and machined in accordance to ASTM E399-08 and ASTM E647-08. Figures 8 and 9 show the recommended configurations of the starter notch and the internal knife-edge. All of the recommended parameters are summarized in the Table 5 as ASTM requirements together with the detail specimen size for this study. The design for the specimen is as illustrated in Figure 10. This fabrication process was conducted using Electrical Discharge Machine (EDM) Wire Cut machine.

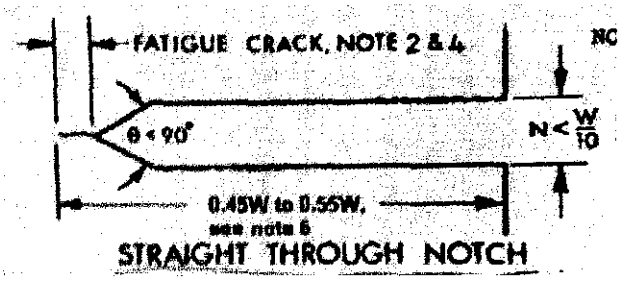

Figure 9: Straight through notch

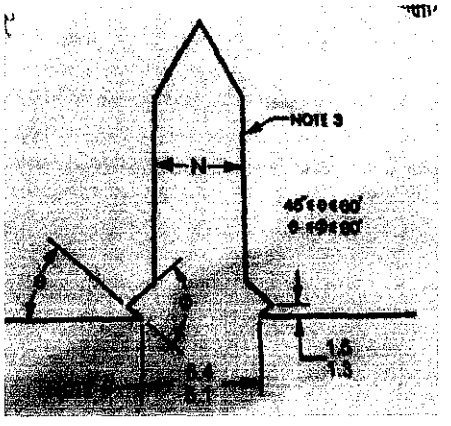

Figure 10: Internal knife edge

Table 6: The configuration of Compact Tension specimen used

Parameter	ASTM Requirement	Fabricated Dimension
Width, W **Thickness, B**	$0.25W < B < 0.5W$ Or alternative specimen: $W/B > 2$	$W = 56$ mm $B = 10$ mm
Crack length, a	$0.45W < a < 0.55W$	25.2 mm< a <30.8 mm
Centers of holes to the plate centerline	$0.75W$	15.4 mm
Holes diameter	$0.25W$	15.28 mm
Notch, N	$N < W/10$	5 mm
Angle of crack starter notch	$\theta < 90^{\circ}$	80°

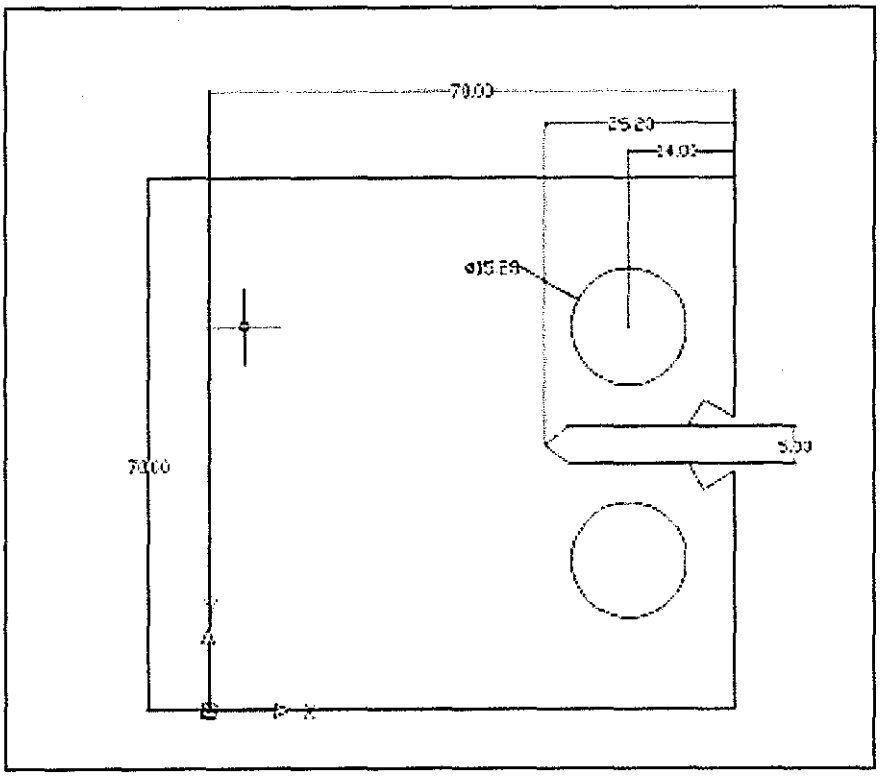

Figure 11: CT Specimen configuration

4.2 Calibration of Extensometer

Prior to performing the tests, the modified extensometer must be first calibrated. The purpose of calibration is to verify the accuracy of the extensometer output, stimulate real-time testing and determine the correction factor of Crack Opening Displacement (COD). A micrometer was used to represent the crack mouth opening for the Crack Opening Displacement.

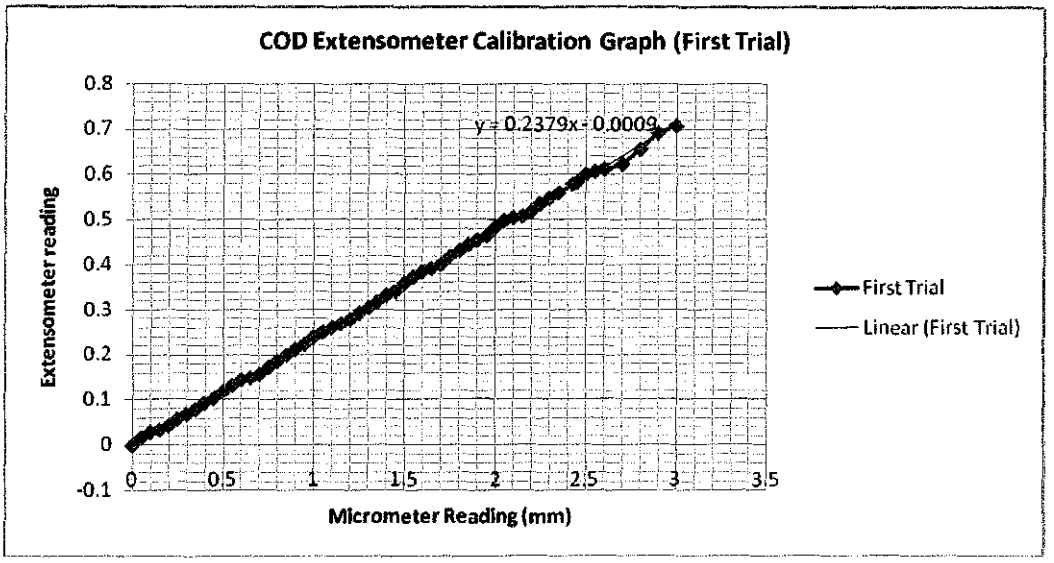

Figure 12: COD extensometer calibration graph (first trial)

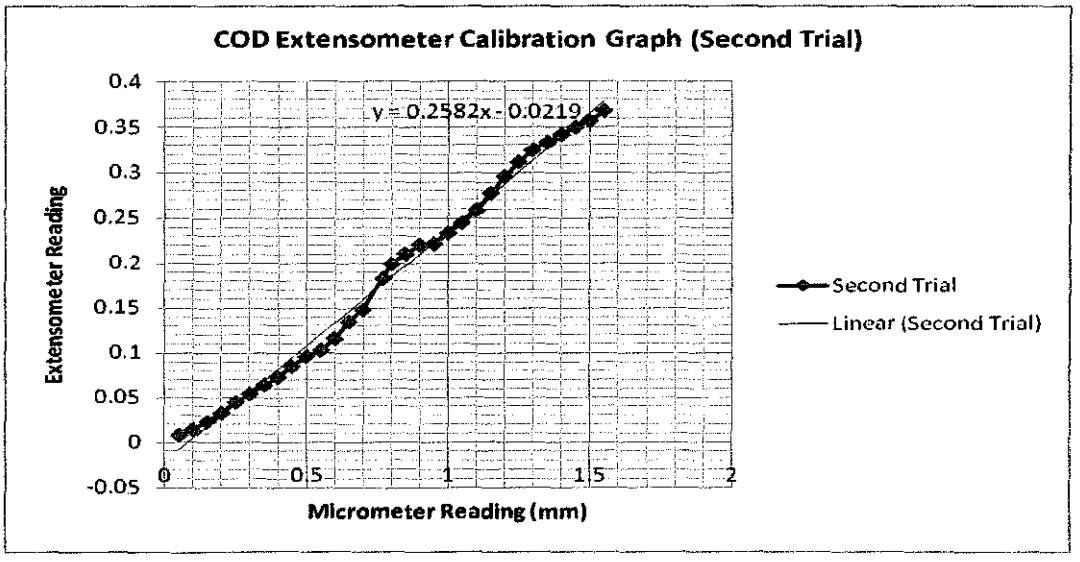

Figure 13: COD extensometer calibration graph (second trial)

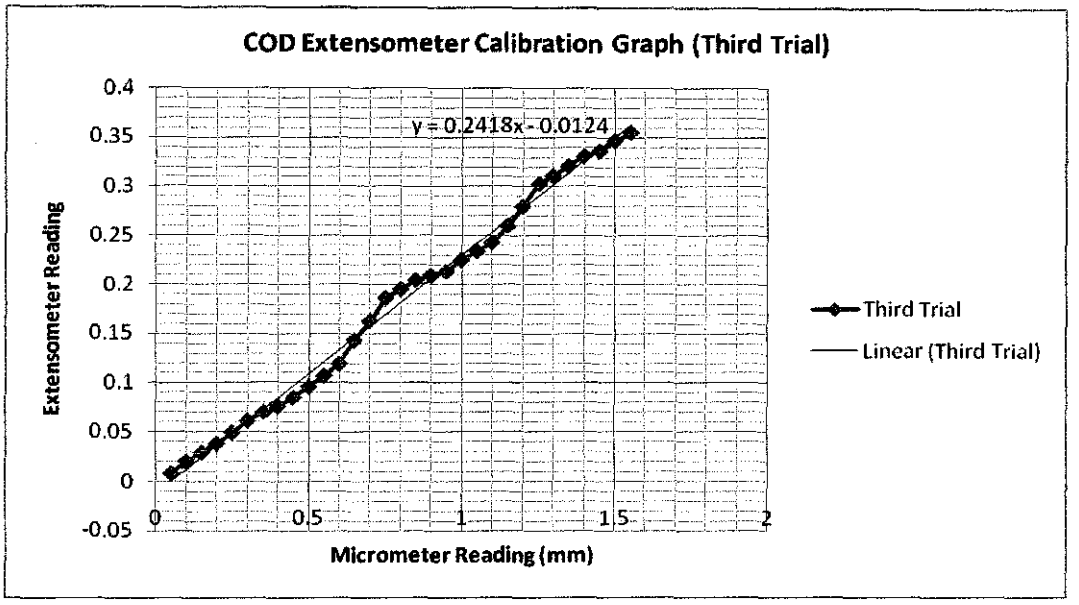

Figure 14: COD extensometer calibration graph (third trial)

From the graphs, the correction factor of COD can be determined by taking average of the graphs gradient:

$$\text{Correction factor} = \frac{0.2379 + 0.2582 + 0.2418}{3} = 0.246.$$

Relationship between micrometer reading (COD) and extensometer reading can be presented as: Extensometer reading = 0.246 x micrometer reading. Therefore, micrometer reading (COD) is 1/0.246 times extensometer reading. In other words:

COD = 4.066 x Extensometer Reading

4.3 Fatigue Precracking

K_{max} for this study ranged from 10% to 80% of K_Q, as shown in Appendix I, assuming that K_Q for NW plate is 50 $MPa\sqrt{m}$. The range of K_Q for FSW plate was assumed to be 50% less than NW plate. Number of cycles for each load increment is summarized in Appendix I. It normally took two days to complete a fatigue-precracking step for each sample. In addition, conducting fatigue precracking for FSW plates was very tough since the crack length behavior of the plate was unpredictable, and it cannot be measured manually using dye penetrant. Hence, trial

and error was used to estimate number of cycles required to precrack for $a \geq 25.5$ mm. Table 6 summarizes the crack length at the end of the precracking stage.

Table 7: Total precrack cycles and corresponding crack length, a of each sample.

Experiment details:	NW				FSW		
	A3	A4	A5	A6	B1	B2	B4
Temperature: 22 – 23°C Humidity: 66 – 68 % Cyclic frequency: 0.3 – 4 Hz Loading: (refer to Appendix I)	Total cycles						
	32850	34000	37610	33586	18000	30000	25000
	Crack length (mm)						
	25.2	25.2	30.0	25.2	-	26.2	22.2

4.4 Fracture Toughness Test

Fracture toughness tests were conducted using stroke rate of 0.01 mm/s. Extensometer and load data were recorded during the tests. Subsequently, graphs of Load (kN) versus Crack Opening Displacement COD (mm) were generated. Values of P_Q were then determined by determine the intercept point of Load vs. COD line with linear lines of 95% slope as illustrated in Appendix II. Figures 14 and 15 show the relationship between load and COD for each sample. K_{IC} values were determined using the mathematical equation below:

$$K_{IC} = \frac{P_{max}\left[f\left(a/W\right)\right]}{B\sqrt{W}}$$

where $P_{max} = P_Q$, B is plate thickness, W is the length from hole's center point to edge of the plate, and $f(a/W)$ is a dimensionless geometry parameter obtained from the equation below:

$$f\left(\frac{a}{W}\right) = \frac{\left(2+\frac{a}{W}\right)\left[0.886+4.64\left(\frac{a}{W}\right)-13.32\left(\frac{a}{W}\right)^2+14.72\left(\frac{a}{W}\right)^3-5.6\left(\frac{a}{W}\right)^4\right]}{\left(1-\frac{a}{W}\right)^{\frac{3}{2}}}$$

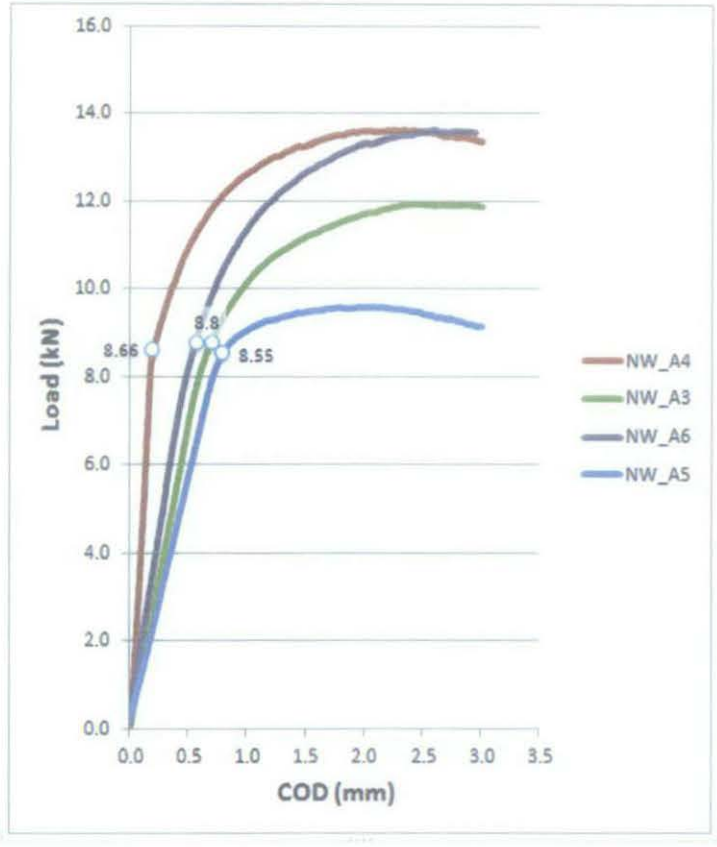

Figure 15: Fracture toughness curves and P_Q values for NW plates

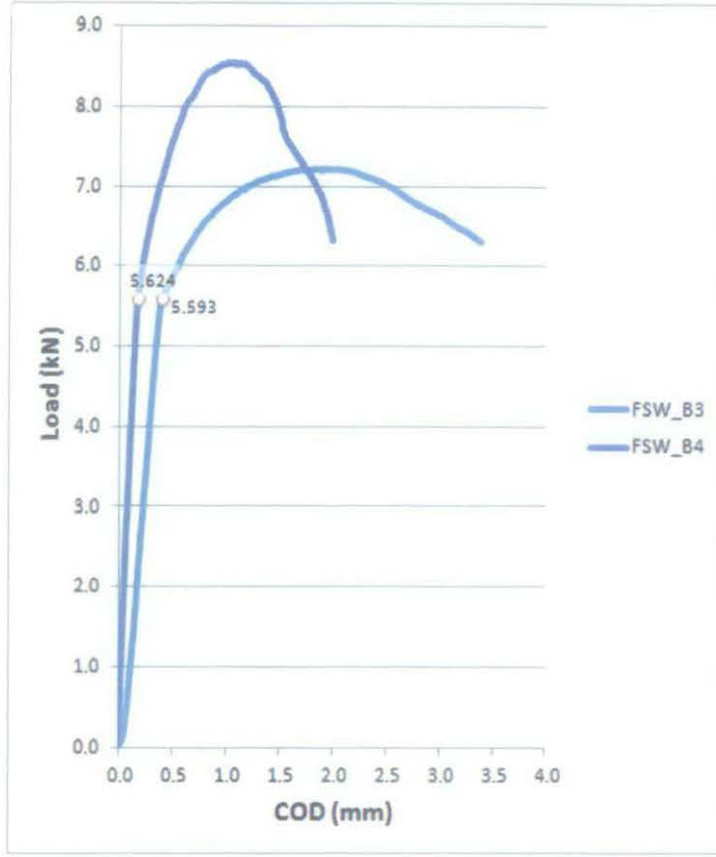

Figure 16: Fracture toughness curves and P_Q values for FSW plates

The summary of the fracture toughness tests is listed in Tables 8, 9, and 10 below.

Table 8: Calculated fracture toughness values, K for both types of plates

Experiment details:	NW				FSW	
	A3	A4	A5	A6	B2	B4
Temperature: 22 – 23°C Humidity: 66 – 68 % Stroke: 0.01mm/s	P_Q (kN)					
	8.80	8.60	8.55	8.80	5.60	5.60
	P_{max} (kN)					
	11.91	13.61	9.57	13.61	7.21	8.54
	$K\,(MPa\sqrt{m})$					
	26.7	26.1	26.0	26.7	17.0	17.0

Table 9: Verification of K_{IC} validity ($P_{max}/P_Q \leq 1.10$)

Sample plate:	P_{max}/P_Q	K_{IC} **Validity requirement:**	**Comment**
NW A3	1.35	$P_{max}/P_Q \leq 1.10$	Not valid
NW A4	1.58		Not valid
NW A5	1.12		Not valid
NW A6	1.55		Not valid
FSW B4	1.53		Not valid
FSW B2	1.29		Not valid

Table 10: Verification of K_{IC} validity ($0.025 \geq 2.5\left(\frac{K_{Ic}}{\sigma_s}\right)^2$)

Sample plate:	$2.5\left(\frac{K_{Ic}}{\sigma_s}\right)^2$	**Validity requirement:**	**Comment**
NW A3	0.114	$0.025 \geq 2.5\left(\frac{K_{Ic}}{\sigma_s}\right)^2$	Not valid
NW A4	0.109		Not valid
NW A5	0.108		Not valid
NW A6	0.114		Not valid
FSW B4	0.046		Not valid
FSW B2	0.046		Not valid

From the plotted graphs, we can see that NW plates yield quite similar values of P_Q with an average of around 8.69 kN. On the other hand, both of FSW plates yield the same P_Q value of 5.60 kN, which is lower than NW samples. Therefore, the calculated stress intensity ratio, K for NW and FSW plates are $26.4\,MPa\sqrt{m}$ and $17.0\,MPa\sqrt{m}$ respectively. This shows that FSW has lower fracture toughness, which is around 60% of NW samples, primarily because of the presence of wormholes along the joint lines. Besides, we can see also that each sample plate behaves differently during loading. The variation in the weld joint itself may contribute to the difference in fracture toughness curve obtained.

Tables 8 and 9 show the results of K_{IC} validity tests, which indicate that the tests failed to comply with K_{IC} validity requirements. This means that the calculated K values are not K_{IC}. This is because plane-strain fracture deals with brittle fracture where it is accompanied by no or little plastic deformation. It is a sensitive property which can only be determined if the sample plates are relatively thick where deformation in z-axis (which is perpendicular to the plate) is small and insignificant, i.e. $\varepsilon_z = 0$.

4.5 Fatigue Crack Growth

Using the same sample configuration and set of test conditions, the relationship between cyclic crack growth rate da/dN and stress intensity range graphs were plotted as illustrated in Figures 16 and 17 to describe the crack growth behaviors for both plates. It has a linear relationship on a log-log plot:

$$\frac{da}{dN} = C(\Delta K)^m$$

$$\log\left(\frac{da}{dN}\right) = m\log(\Delta K) + \log C$$

where m is the slope of the log-log plot and C is a constant. Results for these tests are summarized in Table 10.

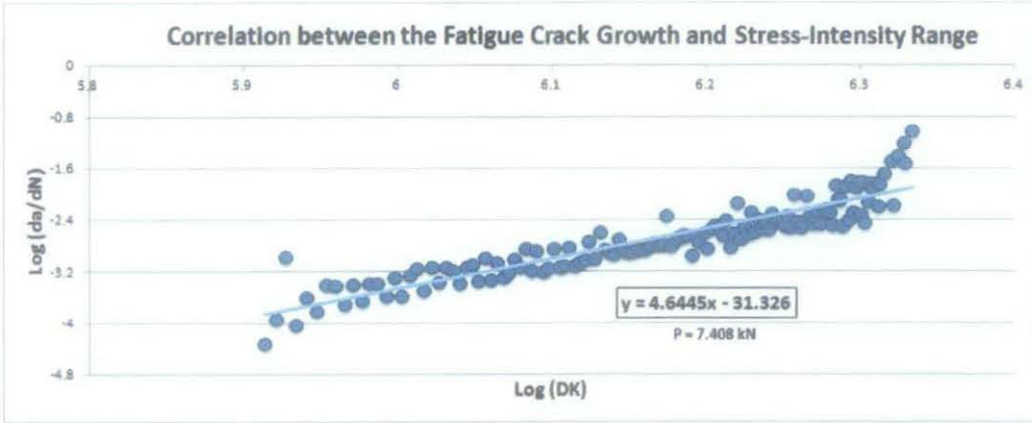

Figure 17: Fatigue crack growth rates versus stress intensities for NW plates

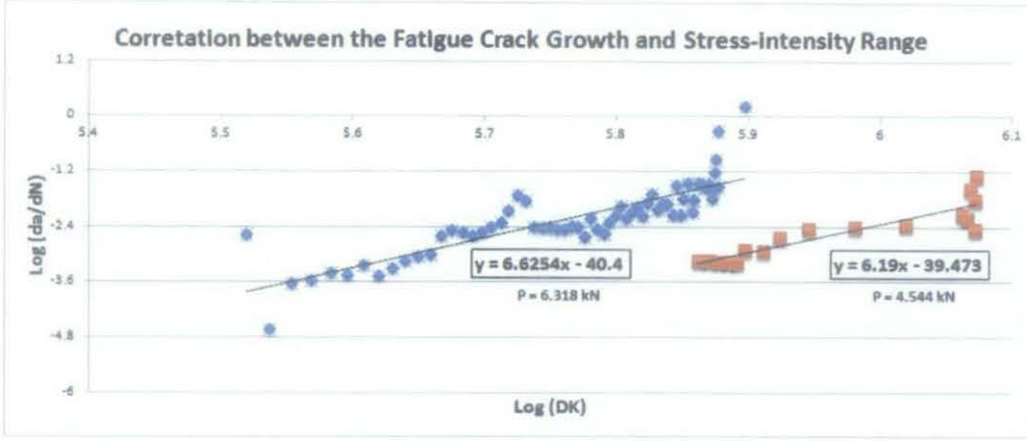

Figure 18: Fatigue crack growth rates versus stress intensities for FSW plates

Table 11: Summary of the FCG test for both types of plates

Experiment details:	NW	FSW	
	C1	D1	D2
Temperature: 22 – 23°C Humidity: 66 – 68 % Stress Ratio: 0.1	Loading (kN)		
	7.408	6.318	4.544
	$C(\frac{mm/cycle}{(MPa\sqrt{m})^m})$		
	4.72×10^{-32}	3.98×10^{-41}	3.37×10^{-40}
	m		
	2.083	6.625	6.190

Since ΔK increases with crack length during constant amplitude loading, and the crack growth rate is dependent on ΔK, the growth rate is not constant but increases with the crack length. Assuming that the effects of environment and frequency are constant, ΔK values during cyclic loading serves the same function as K static loading. It characterized the severity of a combination of loading, geometry and crack length in propagation of cracks. From Table 11, we can see that the FSW has higher value for constant m compared to NW. This indicates that cracks propagate faster in the weld samples or in other words, the FSW sample has lower crack propagation resistance than NW sample.

CHAPTER 5
CONCLUSION

5.1 Conclusion

Fracture Toughness and Fatigue Crack Growth tests for Non-welded and Friction Stir Welded plates using Compact Tension type of sample plate has been successfully completed. Friction stir welded plates were fabricated using the CNC Milling with rotational speed of 1600 rpm, weld speed of 12 mm/min and 12 s dwell time. The welding was performed using tool pin of 8 mm length, 6 mm pin diameter and 12 mm shoulder diameter.

The sample plates were fabricated into CT specimen configuration using Electron Displacement Machine based on ASTM standards. To meet the requirement of sharp notch, precracking was conducted for about 30,000 cycles using a cyclic frequency range of 0.3 - 4.0 Hz with precracked crack lengths of around 25.2 mm. Fracture toughness tests were conducted using 0.01 mm/s stroke rate. Fatigue crack growth tests were conducted using the same cyclic rate range with fatigue precracking, with a stress ratio of 0.1.

Even though the fracture toughness tests did not yield any valid plane-strain fracture toughness value K_{IC}, which represents the minimum fracture toughness where brittle facture will occur, the calculated value of K is a valid fracture toughness of A6061 plate with 10 mm thickness. From the tests, the value of K for friction stir welded plates is nearly 60% lower than the toughness of non-welded plates. In fatigue crack growth tests, friction stir welded plates show nearly similar values of the materials constants m and C. This proved that the relationship between crack growth and load levels did not depend on load levels when the same geometry of components is involved. Furthermore, the welded plates show steeper steady-state crack growth region since m is larger. This verifies that cracks propagate faster in welded plates than in non-welded plates.

5.2 Recommendations

The following are some suggested recommendations for further enhancement of this project:

1. Modify the clevis and COD gage: Fabricate new clevis with better accuracy and reduced tolerance, coupled with the use of a dedicated COD gage and calibrator;

2. Further studies on friction stir welding parameters and pin design: This is to optimize the welding parameters for better fracture toughness and fatigue crack growth properties, instead on just tensile properties;

3. Use thicker specimens: Thicker specimen should be used for FT test although problems in preparing friction stir welded plate must first be addressed;

4. Fractography of fracture surface: Perform microscopy on the surfaces of failed samples to understand the mechanism of failure.

REFERENCES

1. (2008). ASTM E 399 Standard Test Method for Plane-Strain Fracture Toughness of Metallic Materials. In *Annual Books of ASTM Standards.* United States: ASTM International.

2. (2008). ASTM E 647 Standard Test Method for Measurement of Fatigue Crack Growth Rates. In *Annual Books of ASTM Standard.* United States: ASTM International.

3. Dowling, N. (1999). *Mechanical Behavior of Material.* Prentice Hall.

4. Erdogan, E. (2000). Fracture Mechanics. *International Journal of Solids and Structures*, 27, pages 171-183.

5. Fracture Toughness. (2009). Website: http://www.ndt-ed.org/EducationResources/CommunityCollege/Materials/Mechanical/FractureToughness.htm

6. Frantini, L., Pasta, S., & Raynolds, A. (2009). Fatigue crack growth in 2024-T351 friction stir welded joints: Longitudinal residual stress and microstructural effects. *International Journal of Fatigue 31* , 495-500.

7. Friction Stir Welding. Website: http://en.wikipedia.org/wiki/Friction_stir_welding

8. K_{IC} Testing. (2009). Website: http://aluminium.matter.org.uk/content/html/eng/default.asp?catid=176&pageid=2144416586

9. Khodir, S. A., & Toshiya, S. (2007). Microstructure and Mechanical Properties of Friction Stir Welded Similar and Dissimilar Joints of Al and Mg alloys. *Transaction of JWRI* , 27-40.

10. Kulekci, M. K., Kaluc, E., Suk, A., & Basturk, O. (2010). Experimental Comparison of MIG and FSW processes for EN AW 6061-T6 Al Alloy. *The Arabian Journal for Science and Engineering* , 321-330.

11. Kumbhar, N., & Bhanumurthy, K. (2008). Friction Str Welding of Al 6061 Alloy. *Asian J. Exp. Sci.* , 63-74.

12. Mahoney, M., Rhodes, C., Flintoff, J., Spurling, R., & Bingel, W. (1997). Properties of Friction Stir Welded 7075 T651 Aluminium. *Metallurgical and Material Transactions A.*

13. Moreira, P., Jesus, A., Ribeiro, A., & Castro, P. (2008). Fatigue Crack Growth Behaviour of the Friction Stir Welded 6082-T6 Aluminium Alloy. *Mecanica Experimental*, 99-106.

14. Pirondi, A., Collini, L., & Fersini, D. (2008). Fracture and fatigue crack growth behaviour of PMMC friction stir welded butt joints. *Engineering Fracture Mechanics 75*, 4333-43

15. Sivashanmugan, M., Ravikumar, S., Rao, V. S., Muruganandam, D., & Kumar, T. (2010). A Review on Friction Stir Welding for aluminium alloys. 216-221.

Fatigue Precracking

Stage 1

Kq= 50 Mpa
a2= 0.02 m
W= 0.056 m

$$f\left(\frac{a}{W}\right)=\frac{\left(2+\frac{a}{W}\right)\left[0.886+4.64\left(\frac{a}{W}\right)-13.32\left(\frac{a}{W}\right)^{2}+14.72\left(\frac{a}{W}\right)^{3}-5.6\left(\frac{a}{W}\right)^{4}\right]}{\left(1-\frac{a}{W}\right)^{\frac{3}{2}}}$$

Therefore,
f(a/W)= 6.5104

$$P=\frac{K_Q B\sqrt{W}}{f\left(\frac{a}{W}\right)}$$

%	Max load(kN)	Min load (kN)
100%=	18.174	
80%=	14.539	1.454
75%=	13.631	1.363
70%=	12.722	1.272
65%=	11.813	1.181
60%=	10.905	1.090
55%=	9.996	1.000
50%=	9.087	0.909
45%=	8.178	0.818
40%=	7.270	0.727
35%=	6.361	0.636
30%=	5.452	0.545
25%=	4.544	0.454
20%=	3.635	0.363
15%=	2.726	0.273
10%=	1.817	0.182

Stage 2

Kq= 50 Mpa
a2= 0.0252 m
W= 0.056 m

Therefore,
f(a/W)= 7.1876

$$P=\frac{K_Q B\sqrt{W}}{f\left(\frac{a}{W}\right)}$$

%	Max load(kN)	Min load (kN)
100%=	16.462	
80%=	13.170	1.317
75%=	12.347	1.235
70%=	11.523	1.152
65%=	10.700	1.070
60%=	9.877	0.988
55%=	9.054	0.905
50%=	8.231	0.823
45%=	7.408	0.741
40%=	6.585	0.658
35%=	5.762	0.576
30%=	4.939	0.494
25%=	4.116	0.412
20%=	3.292	0.329
15%=	2.469	0.247
10%=	1.646	0.165

Figure 7.1: Maximum and minimum precracking loads for NW Plates

Fatigue Precracking

Kq= 25 Mpa
a1= 0.02 m
W= 0.056 m

$$f\left(\frac{a}{W}\right)=\frac{\left(2+\frac{a}{W}\right)\left[0.886+4.64\left(\frac{a}{W}\right)-13.32\left(\frac{a}{W}\right)^{2}+14.72\left(\frac{a}{W}\right)^{3}-5.6\left(\frac{a}{W}\right)^{4}\right]}{\left(1-\frac{a}{W}\right)^{\frac{3}{2}}}$$

Therefore,

f(a/W)= 6.5104

$$P=\frac{K_{Q}B\sqrt{W}}{f\left(\frac{a}{W}\right)}$$

%	Max load(kN)	Min load (kN)
100%=	9.087	
80%=	7.270	0.727
75%=	6.815	0.682
70%=	6.361	0.636
65%=	5.907	0.591
60%=	5.452	0.545
55%=	4.998	0.500
50%=	4.544	0.454
45%=	4.089	0.409
40%=	3.635	0.363
35%=	3.181	0.318
30%=	2.726	0.273
25%=	2.272	0.227
20%=	1.817	0.182
15%=	1.363	0.136
10%=	0.909	0.091

Figure 7.2: Maximum and minimum precracking loads for FSW Plates

STAGE 1

Loading (kN)		No of Cycles (Sample)					
P(max)	P(min)	A1	A2	A3	A4	A5	A6
7.07	0.707	3000	3000	3000	3000	3000	3000
7.270	0.727	2000	2000	3000	3000	3000	3000
8.178	0.818	1600		3000	3000	3000	3000
9.087	0.909			3000	3000	3000	3000
9.996	1.000	TRIAL		3000	3000	3000	3000
10.905	1.091			3000	3000	3000	3000
11.813	1.1813				2000	2000	2000
				18000	20000	20000	20000

STAGE 2

Loading (kN)		No of Cycles (Sample)					
P(max)	P(min)	A1	A2	A3	A4	A5	A6
4.939	0.494			3000	3000	3000	3000
5.762	0.576			3000	3000	3000	3000
6.585	0.658	TRIAL		3000	3000	3000	2000
7.408	0.741			3000	5000	3000	3020
8.231	0.823			2850		3000	2566
9.054	0.905					2610	
				14850	14000	17610	13586
				32850	34000	37610	33586

Figure 7.3: Number of cycles for each load increment (NW)

Loading (kN)		No of Cycle (Sample)			
P(max)	P(min)	B1	B2	B3	B4
1.817	0.182	3000	3000	3000	3000
2.272	0.227		3000	3000	
2.726	0.273	3000	3000	3000	3000
3.181	0.318		3000	3000	
3.635	0.363	3000	3000		3000
4.089	0.409		3000		
4.544	0.454	3000	3000		5000
4.998	0.500		3000		5000
5.452	0.545	3000	3000		5000
5.907	0.591		3000		3000
6.361	0.636	3000			
		18000	12000	12000	24000
		failed!		Broken!	

Figure 7.4: Number of cycles for each load increment (FSW)

APPENDIX II

Fracture Toughness Test

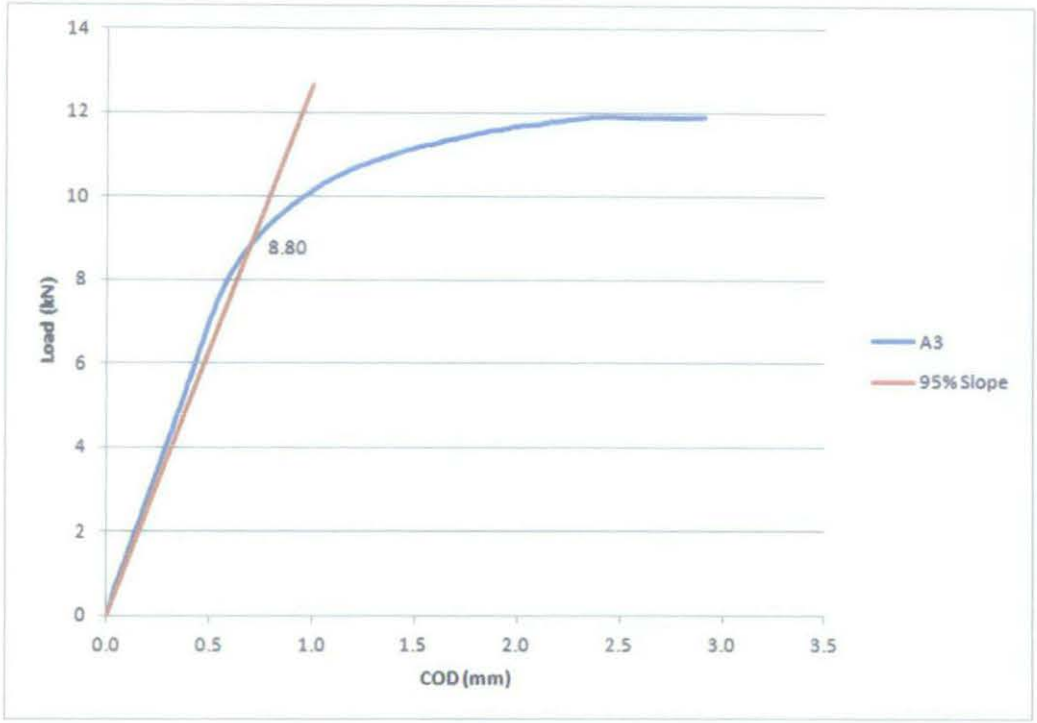

Figure 7.5: Load vs COD with 95% slope intercept (NW A3)

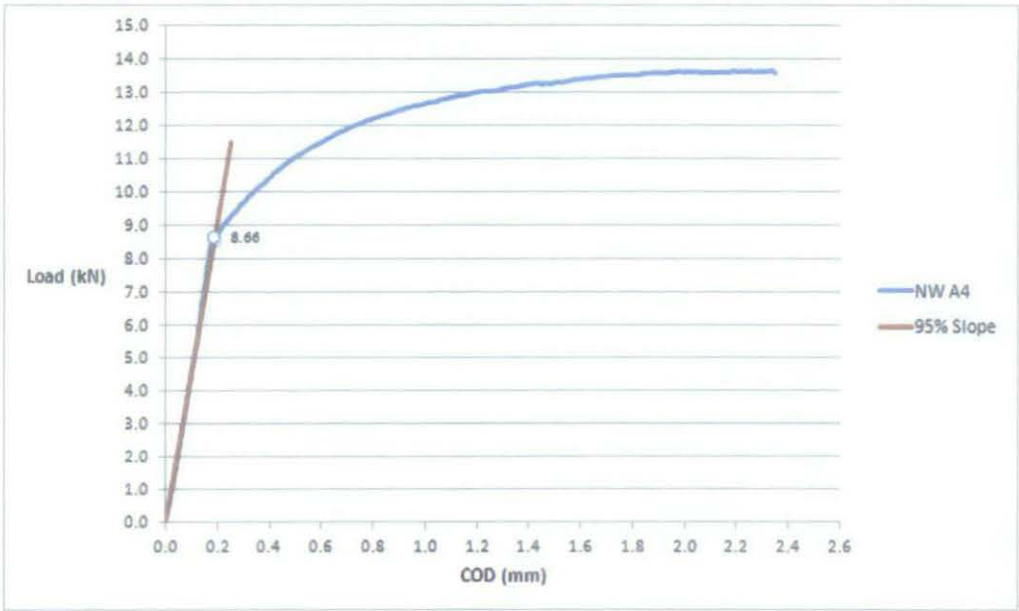

Figure 7.6: Load vs COD with 95% slope intercept (NW A4)

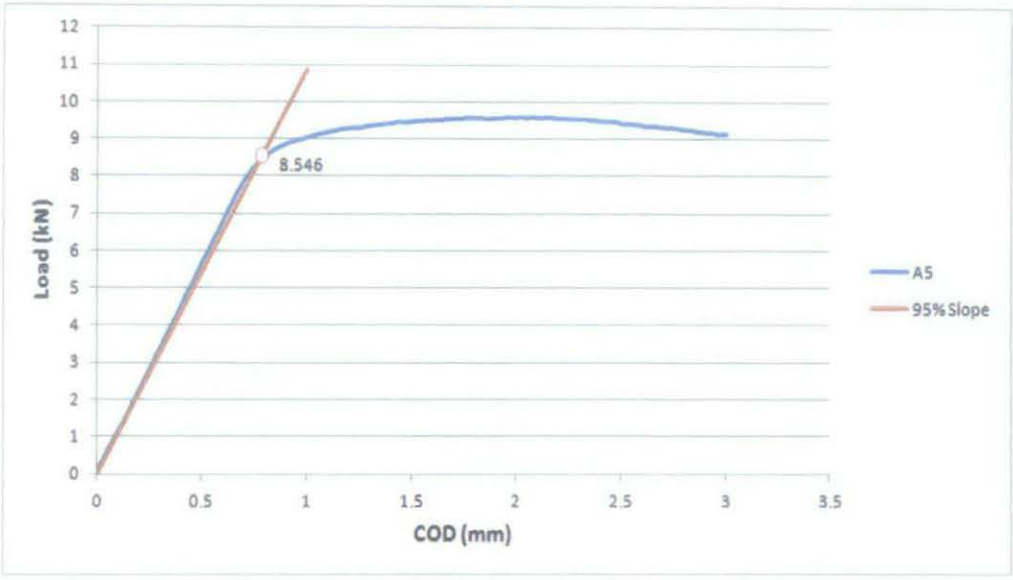

Figure 7.7: Load vs COD with 95% slope intercept (NW A5)

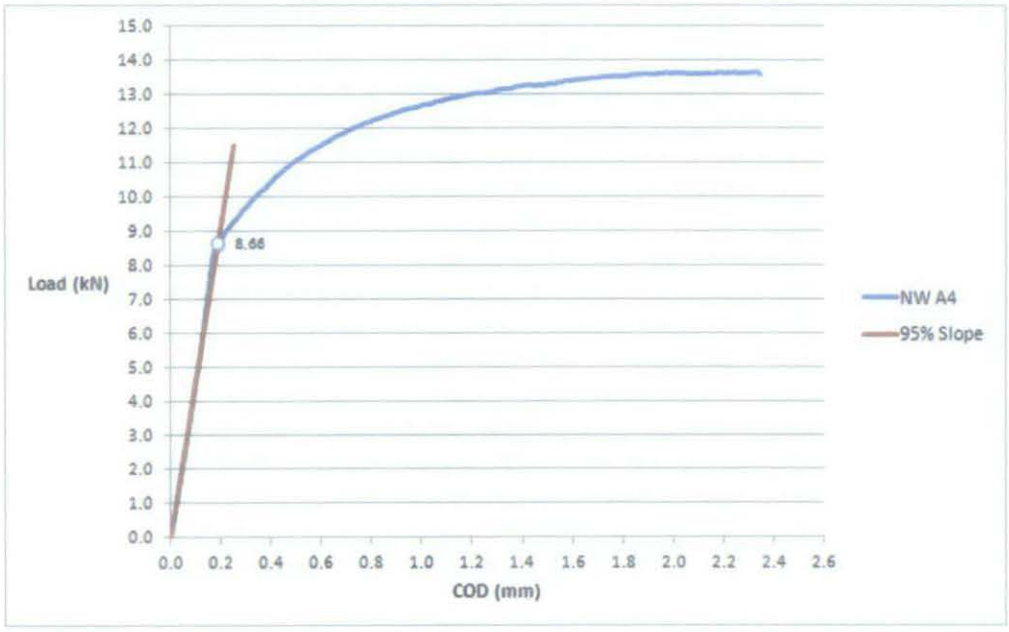

Figure 7.8: Load vs COD with 95% slope intercept (NW A6)

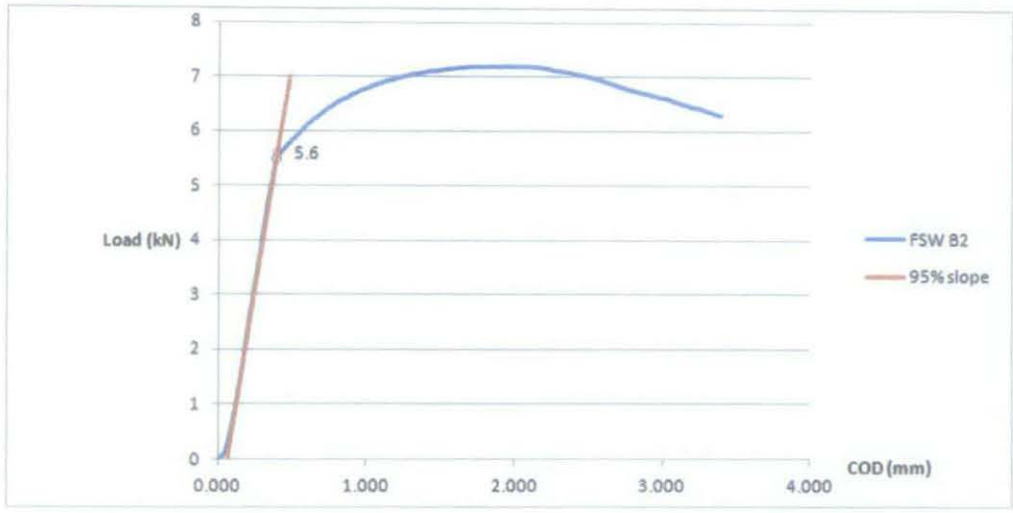

Figure 7.10: Load vs COD with 95% slope intercept (FSW B2)

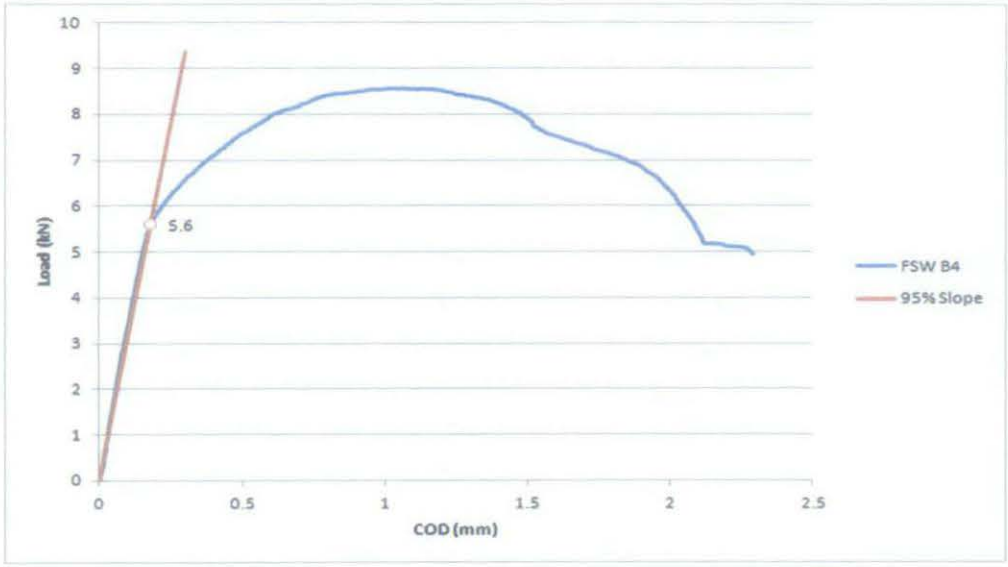

Figure 7.9: Load vs COD with 95% slope intercept (FSW B4)